Backwater and river plume controls on scour upstream of river mouths: Implications for fluvio-deltaic morphodynamics

Michael P. Lamb,[1] Jeffrey A. Nittrouer,[2] David Mohrig,[3] and John Shaw[3]

Received 5 May 2011; revised 6 October 2011; accepted 10 October 2011; published 7 January 2012.

[1] Sediment flux from rivers to oceans is the fundamental driver of fluvio-deltaic morphodynamics and continental margin sedimentation, yet sediment transport across the river-to-marine boundary is poorly understood. Coastal rivers typically are affected by backwater, a zone of spatially decelerating flow that is transitional between normal flow upstream and the offshore river plume. Flow deceleration in the backwater zone, as well as spreading of the offshore plume, should render rivers highly depositional near their mouths, leading to sedimentation and eventual elimination of the backwater zone at steady state. This reasoning is counter to observations of riverbed scour, erosional bed forms, and long-lived backwater zones near the mouths of some coastal rivers (e.g., Mississippi River, United States). To explain these observations, we present a quasi-2-D model of a coupled fluvial backwater and offshore river plume system and apply it to the Mississippi River. Results show that during high-discharge events the normal-flow depth can become larger than the water depth at the river mouth resulting in drawdown of the water surface, spatial acceleration of flow, and erosion of the riverbed. As proposed by Lane (1957), the transition to drawdown and erosion is ultimately forced by spreading of the offshore river plume. This points to the need to model coupled river and river plume systems with a dynamic backwater zone under a suite of discharges to accurately capture fluvio-deltaic morphodynamics and connectivity between fluvial sediment sources and marine depositional sinks.

Citation: Lamb, M. P., J. A. Nittrouer, D. Mohrig, and J. Shaw (2012), Backwater and river plume controls on scour upstream of river mouths: Implications for fluvio-deltaic morphodynamics, *J. Geophys. Res.*, *117*, F01002, doi:10.1029/2011JF002079.

1. Introduction

[2] Sediment flux from rivers to the ocean is the main driver of continental sedimentation with significant implications for land use, construction of hydrocarbon reservoirs, and unraveling Earth history and global climate change from sedimentary strata [e.g., *Nittrouer*, 1999; *Blum and Törnqvist*, 2000; *Paola*, 2000; *Paola et al.*, 2011]. Much of the world's population lives near river mouths and deltas, areas vulnerable to catastrophic inundation from river floods, tsunamis, hurricanes, subsidence, and global sea level rise, all of which are extremely sensitive to changes in land surface elevations produced by imbalances in sediment flux [e.g., *Syvitski and Saito*, 2007; *Syvitski et al.*, 2009]. River mouths represent a fundamental transition in the sediment source-to-sink pathway where rivers hand off to marine transport processes. Despite the importance of this transfer, there exists considerable uncertainty about the controls on erosion and deposition of sediment near river mouths [e.g., *Blum and Törnqvist*, 2000; *Fagherazzi et al.*, 2004; *Sylvia and Galloway*, 2006; *Törnqvist et al.*, 2006; *Mattheus et al.*, 2007; *Parker et al.*, 2008b].

[3] Rivers behave fundamentally differently near their mouths than farther upstream because they are affected by the static water beyond the shoreline. This affected zone is known as the backwater and can be expansive for large, low-sloping rivers, creating nonuniform flow that decelerates toward the river mouth (Figure 1). For example, during low-flow conditions on the Mississippi River, United States, the backwater zone extends ~500 km upstream of the river mouth [e.g., *Nittrouer et al.*, 2011b; *Parker et al.*, 2009]. The backwater zone is dynamic, however, and its upstream extent is sensitive to river discharge as well as the water surface elevation at the river mouth, which in turn can be affected by sea level, storm surge, tides, and river plume dynamics, for example. During large floods the upstream boundary of backwater can be pushed toward the shoreline altering the spatial convergence of sediment flux that ultimately controls erosion and deposition patterns [*Hoyal and Sheets*, 2009; *Lamb and Mohrig*, 2009; *Nittrouer et al.*, 2011b].

[4] Although backwater hydrodynamics have been studied for some time [e.g., *Chow*, 1959], little work has explored the effects of a dynamic backwater zone on sediment transport, channel dynamics, and bathymetric evolution. Indeed, many morphodynamic models employ topographic diffusion

[1]Division of Geological and Planetary Sciences, California Institute of Technology, Pasadena, California, USA.
[2]Department of Geology, University of Illinois at Urbana-Champaign, Urbana, Illinois, USA.
[3]Jackson School of Geosciences, University of Texas, Austin, Texas, USA.

0148-0227/12/2011JF002079

This article was corrected on 12 OCT 2015. See the end of the full text for details.

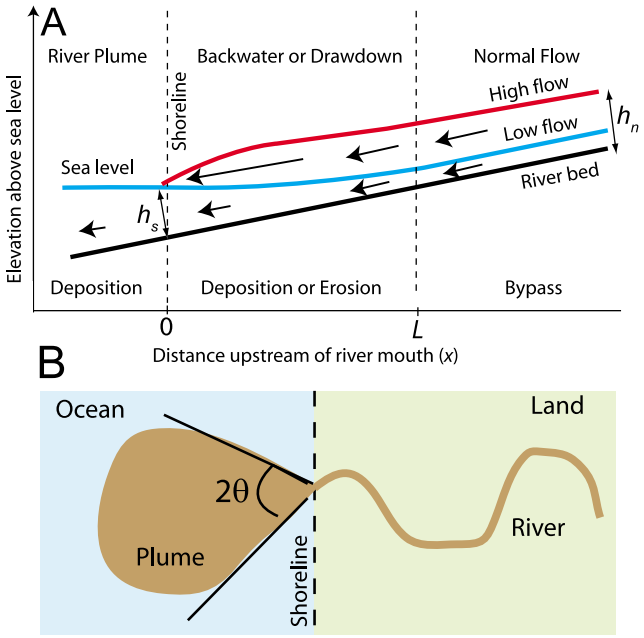

Figure 1. Cartoon showing a river entering an ocean with three zones of interest: normal flow ($x > L$), a transitional region ($0 < x < L$), and the offshore river plume ($x < 0$) in (a) cross section and (b) plan view. As shown in Figure 1a, at low flow the transitional region is a zone of backwater, where the water depth at the shoreline (h_s) is greater than the normal flow depth (h_n), and the water surface (blue) and bed (black) diverge downstream (i.e., M1 curve [e.g., *Chow*, 1959]) resulting in deceleration (shown by length of arrows) and deposition. At high flow $h_n > h_s$ and the water surface (red) is convex (i.e., M2 curve [e.g., *Chow*, 1959]), resulting in spatial acceleration of flow and erosion. In both cases, the elevation of the water surface at the river mouth is relatively insensitive to discharge due to lateral spreading of the plume. After *Lane* [1957].

[e.g., *Flemings and Jordan*, 1989; *Paola et al.*, 1992; *Swenson et al.*, 2005], which implicitly assumes steady and uniform flow and neglects backwater effects. Physical experiments have minimized or eliminated backwater effects because of relatively steep bed slopes and large Froude numbers in comparison to natural rivers [*Muto*, 2001; *Sheets et al.*, 2002; *Swenson and Muto*, 2007; *Parker et al.*, 2008b; *Hoyal and Sheets*, 2009]. Only a few models exist that have incorporated a backwater zone in basin filling [*Chang*, 1982; *Snow and Slingerland*, 1987; *Hotchkiss and Parker*, 1991; *Slingerland et al.*, 1994; *Hoyal and Sheets*, 2009] and fluvial response to relative sea level [*Parker et al.*, 2008a], but these assume that morphodynamics are governed by a characteristic discharge and therefore neglect variable flood discharges that make the backwater zone dynamic.

[5] Backwater, combined with rapid spreading of flow beyond the shoreline, should render rivers near their mouths highly depositional. Recent work on the lower Mississippi River contradicts this intuition, demonstrating that a large portion of the river bed (25 to 40%) in the final 165 km consists of substrate devoid of active alluvial cover [*Nittrouer et al.*, 2011a]. The substrate is exposed in the channel thalweg, particularly in bend segments, and displays features such as flutes, potholes, and large scours that indicate active erosion by sediment abrasion [*Whipple et al.*, 2000] and fluid flow [*Allen*, 1971]. Bathymetric surveys on other river deltas (e.g., Wax Lake, United States) also show, in some cases, scour in a region upstream of river bifurcations [e.g., *Galler et al.*, 2003; *Shaw and Mohrig*, 2009]. Evidently rivers can erode as well as deposit sediment in fluvial backwater zones, a dynamic which is currently neglected in source-to-sink and stratigraphy generation models. Can backwater dynamics explain such erosion in the final reaches of rivers?

[6] With a single characteristic discharge and in the absence of delta progradation, backwater regions should aggrade until the depth and slope adjust to create normal-flow and sediment bypass conditions at steady state (e.g., G. Parker, 1-D sediment transport morphodynamics with applications to rivers and turbidity currents, University of Illinois at Urbana-Champagne, 2004, available at http://vtchl.uiuc.edu/people/parkerg/1106powerpoint_lectures.htm, hereinafter online book, 2004). Thus, many backwater zones and estuaries are interpreted to be transient features that result from flooding due to Holocene sea level rise that created accommodation space faster than could be balanced by fluvial sediment infilling [e.g., *Anderson and Rodriguez*, 2008]. This notwithstanding, many rivers have backwater zones that persist despite the formation of Holocene highstand deltas (e.g., Mississippi River, United States). This suggests that backwater dynamics may be important in shaping channel morphology through deposition *and erosion*.

[7] *Lane* [1957] argued that the lowermost portions of rivers can become erosional at high discharges due to drawdown of the fluvial water surface near the river mouth and spatial acceleration of the flow toward the shoreline, in contrast to deceleration observed at low flow. Key to this hypothesis is that lateral spreading of the river plume beyond the shoreline renders the water surface there relatively fixed in elevation (Figure 1). Although lateral spreading is most often linked to spatial deceleration and deposition, its effect on water surface elevation may result in drawdown and scour upstream of river mouths during large flood events. If Lane's hypothesis is correct, it indicates that river mouths can be zones of erosion during high-discharge events, and it points to the need to model river and river plumes as coupled systems with a dynamic backwater zone under a suite of discharges to accurately capture topographic evolution and sediment transport dynamics.

[8] Herein, we explore *Lane*'s [1957] hypothesis by first presenting it as a conceptual model and second as a quasi-2-D numerical model that couples fluvial backwater hydrodynamics with an offshore spreading river plume. We find the hypothesis to be a reasonable explanation for scour near river mouths of large, low-sloping rivers. To test the hypothesis, we compare the model against topographic, stage height and velocity data for the lower Mississippi River. Last, we discuss the implications for the channel-forming discharge hypothesis, source-to-sink sediment transport, river plume dynamics, and fluvio-deltaic morphodynamics.

2. Drawdown Hypothesis

[9] *Lane* [1957] observed that many rivers including the Mississippi River and those that enter the Great Lakes of

North America are much deeper near their mouths than farther upstream. He reasoned that this must be the result of infrequent large flow events that focus scour near river mouths. The scour, he proposed, results from drawdown of the water surface elevation near the river mouth during flood because the water surface within the receiving basin is relatively fixed (Figure 1).

[10] Following *Lane* [1957], we illustrate the drawdown hypothesis under the simplest scenario possible that still incorporates the appropriate physics. For a river of uniform width and constant bed slope entering an unconfined ocean basin there are three main hydrodynamic zones of interest: normal flow, backwater, and the river plume beyond the shoreline (Figure 1a). The effects of waves, tides, ocean currents, the Coriolis force, density stratification, and buoyancy (e.g., that influences hyperpycnal or hypopycnal behavior) are neglected. The normal flow zone ($x > L$, where $x = 0$ is at the river mouth and L is the upstream extent of backwater) is a region of uniform flow where the water surface parallels the bed (Figure 1a). If temporal changes in flow dynamics and lateral sediment supply inputs can be neglected, the normal-flow zone is a region of sediment bypass. Beyond the shoreline, river plumes often spread laterally due to the loss of confinement (Figure 1b), which in general causes spatial deceleration and deposition [e.g., *Wright*, 1977; *Geyer et al.*, 2004; *Falcini and Jerolmack*, 2010; *Rowland et al.*, 2010].

[11] Normal river flow and the offshore river plume are connected by a transitional zone ($0 < x < L$), the spatial extent and hydrodynamics of which are sensitive to the upstream, downstream and bottom boundary conditions. At low flow, the transitional zone has a concave water surface profile because the water depth at the shoreline (h_s) is greater than the normal-flow depth (h_n) due to a fixed sea level (i.e., it is a backwater zone, with a so-called M1 profile [*Chow*, 1959]) (Figure 1a). This creates a zone of spatial deceleration and deposition. In contrast, at high flows the transitional zone can become a region of flow acceleration and erosion if the water depth at the shoreline is less than the normal flow depth (i.e., it is drawdown zone, with a so-called M2 profile [*Chow*, 1959]) (Figure 1a).

[12] *Lane* [1957] recognized that drawdown of the water surface profile and focused scour just upstream of the river mouth require the water surface within the receiving basin to be relatively fixed in elevation: "If the lake level should rise rapidly as the flood enters it, the drop down curve might be too small to produce sufficient scour…" [*Lane*, 1957, p. 94]. By continuity, the relative insensitivity of the offshore water surface elevation to river discharge is due to the great expansion of the cross-sectional area of flow there (Figure 1b). Thus, under the geometric assumptions stated, if river discharge is sufficiently large to increase flow depth in the normal flow zone and lateral spreading is sufficiently large so that the water surface elevation is relatively fixed near sea level, then river flow will be forced to thin and accelerate in the downstream direction to match the water surface elevation at the river mouth. In section 4, we test this hypothesis using a quasi-2-D hydrodynamic model and evaluate it for the case of the Mississippi River.

3. Model Development

[13] The controls on erosion and deposition near river mouths can be explored using a quasi-2-D formulation for conservation of fluid mass and momentum, and conservation of sediment mass. The discharge of water is steady across the model domain and time-dependent processes (e.g., flood waves and topographic evolution of the bed) are neglected in our model for simplicity. We model sediment transport only to identify zones of erosion and deposition.

[14] The hydrodynamic model for river flow is based on conservation of fluid mass and momentum for depth-averaged, gradually varied flow in the streamwise (x) direction [*Chow*, 1959]. Lateral changes in the cross-sectional area of the flow are accounted for in continuity only and are neglected in the momentum equation. Following these assumptions [e.g., *Chow*, 1959],

$$\frac{dh}{dx} = \frac{S_b - C_f F^2}{1 - F^2}, \tag{1}$$

where h is the thalweg depth, S_b is the bed slope, C_f is a dimensionless coefficient of friction, $F = \left(\frac{Q^2 B}{gA^3}\right)^{1/2}$ is the Froude number, B is the top width of the wetted channel, A is the cross-sectional area of flow, $Q = UA$ is the volumetric flux of water, U is the average flow velocity in the x direction, and g is the acceleration due to gravity. The normal flow depth can be recovered from equation (1) by setting $dh/dx = 0$, resulting in $h_n = (C_f Q^2 B / g S_b w^3)^{1/3}$ [e.g., *Chow*, 1959], where $w = A/h$ is the depth-averaged width of flow.

[15] Offshore, river plumes tend to spread laterally and sometimes vertically due to loss of river channel confinement and this is an effect we want to incorporate into our model. River plume spreading can be affected by river velocity, channel width-to-depth ratio, bed friction, mixing and the associated drag along the lateral margins of the plume [e.g., *Rajaratnam*, 1976; *Wright*, 1977; *Rowland et al.*, 2009], levees and mouth bars [e.g., *Wright*, 1977; *Edmonds and Slingerland*, 2007; *Falcini and Jerolmack*, 2010; *Rowland et al.*, 2010], waves, wind, tides, and other oceanic currents [e.g., *Lamb et al.*, 2008; *Schiller et al.*, 2011]. Fluid density differences between the plume and the receiving basin can cause the plume to plunge beneath the basin water (i.e., a hyperpycnal plume) [e.g., *Bates*, 1953; *Mulder and Syvitski*, 1995; *Geyer et al.*, 2004; *Lamb et al.*, 2010] or detach from the bed to become a buoyant hypopycnal plume. The latter is typically steered by the Coriolis force which can lead to an anticyclonic eddy of freshwater (or bulge) near the river mouth in some cases [e.g., *Kourafalou et al.*, 1996; *Fong and Geyer*, 2002; *Horner-Devine et al.*, 2006; *Horner-Devine*, 2009; *Schiller and Kourafalou*, 2010]. Incorporating the dynamics of these river plume processes in a rigorous way is beyond the scope of our study.

[16] For our purposes, we seek to incorporate the effect that the water surface elevation at the river mouth is relatively insensitive to changes in river discharge as compared to farther upstream due to the effects of lateral spreading, entrainment, and buoyancy. For example, stage height increases by <1 m at the mouth of the Mississippi River during large floods, whereas stage heights can increase by >10 m further upstream [e.g., *Karadogan et al.*, 2009]. In

general, positively buoyant plumes tend to have relatively small water surface elevation anomalies ($\ll$1 m) [e.g., *McCabe et al.*, 2009].

[17] The simplest way to incorporate the effect of lateral plume spreading would be to force the water surface elevation at the river mouth to be at sea level through use of a boundary condition at $x = 0$ in equation (1) [e.g., *Parker et al.*, 2008a; *Karadogan et al.*, 2009]. We have found, however, that forcing the water surface to sea level at $x = 0$ is too restrictive and can produce a drawdown effect that is greater than observed. To allow for some variation of the water elevation surface at the river mouth, we instead treat the offshore plume as a depth-averaged, steady, homopycnal current, where momentum is balanced in 1-D between a hydrostatic pressure gradient and drag along the bed (i.e., equation (1)). We neglect drag and entrainment along the lateral margins of the plume and represent lateral spreading of the plume geometrically by assigning a set spreading angle (θ) beyond the shoreline ($x < 0$). Thus, in equation (1), $A = wh$ and the average width of the plume beyond the shoreline (i.e., $x < 0$) is calculated from $\frac{dw}{dx} = 2\tan\theta$ where θ is the spreading angle of the plume relative to the center streamline (Figure 1b). Theory, experiments, and field observations have found that spreading angle tends to be $\sim$5 to 13 degrees [e.g., *Wright and Coleman*, 1971; *Rajaratnam*, 1976; *Wang*, 1984; *Falcini and Jerolmack*, 2010; *Rowland et al.*, 2010]. Although our representation of the plume is highly simplified, it is sufficient to reproduce the desired effect of a dynamic river mouth water surface elevation that is a model outcome (rather than a boundary condition) and is controlled by the independent parameters of river discharge and plume spreading angle.

[18] For some rivers, flow passes through a series of deltaic bifurcations before entering the open ocean. Our quasi-2-D formulation is not capable of accurately simulating flow through bifurcations. In such a case, we set $x = 0$ to be the location of the first major bifurcation rather than the shoreline. A bifurcation, like an unconfined plume, can result in a net increase in channel cross-sectional area [*Edmonds and Slingerland*, 2007; *Shaw and Mohrig*, 2009], and therefore may induce enough spreading to cause M2 behavior upstream at high flow.

[19] To solve equation (1), the bed elevation, channel cross section, and discharge are specified everywhere along the flow path. For subcritical flow ($F < 1$) considered here, the water level in the basin is fixed at sea level very far downstream of the region of interest ($x \ll 0$), which allows a dynamic water surface elevation at the river mouth (i.e., there is no boundary condition set at $x = 0$). The calculation for flow depth proceeds in an upstream direction from this boundary condition using a second-order finite difference scheme applied to equation (1).

[20] To identify zones of erosion and deposition, we assume dilute flow and conserve sediment mass using

$$\frac{d\eta}{dt} = -\frac{1}{1-\lambda_p}\frac{1}{w}\frac{dQ_s}{dx}, \tag{2}$$

where η is the elevation of the bed, λ_p is the bed porosity, and Q_s is the volumetric sediment flux. The volumetric sediment flux is calculated assuming sediment transport capacity using the total load formula of *Engelund and Hansen* [1967],

$$Q_s = w\left(RgD_{50}{}^3\right)^{1/2}\left(\frac{0.05}{C_f}\right)\tau_*^{5/2}, \tag{3}$$

where R is the submerged specific density of the sediment ($\sim$1.65), D_{50} is the median grain diameter, $\tau_* = \frac{u_*^2}{RgD_{50}}$ is the Shields stress, and $u_* = \sqrt{C_f U^2}$ is the shear velocity. After calculating the hydrodynamics using equation (1), the resultant flow velocity (U) is combined with equations (2) and (3) to estimate the rates of erosion and deposition (i.e., $\frac{d\eta}{dt}$). Form drag due to bed forms is implicitly accounted for in equation (3) through C_f [*Engelund and Hansen*, 1967].

4. Model Results

[21] The model and concepts presented herein are meant to be applicable to coastal rivers in general. However, it is useful to explore the model results using parameters that scale roughly after a natural river. Here we choose the Mississippi River because it is a large lowland river where backwater and sediment dynamics have been investigated [*Carey and Keller*, 1957; *Lane*, 1957; *Parker et al.*, 2009; *Nittrouer et al.*, 2011b], scour near the river mouth has been observed [*Nittrouer et al.*, 2012], and there exists a wide range of data with which to compare model predictions [e.g., *Harmar et al.*, 2005]. We know of no other coastal river where such detailed data within the backwater zone are publicly available.

[22] Backwater hydraulics has been argued to play an important role in the transport of bed material sediment in the lower Mississippi River [e.g., *Carey and Keller*, 1957; *Lane*, 1957; *Wright and Parker*, 2004; *Parker et al.*, 2009; *Nittrouer et al.*, 2011b]. *Nittrouer et al.* [2012] showed that during low-water discharge ($Q < 10^4$ m^3/s), water velocity and shear stress decrease progressing from where normal-flow conditions persist toward the river outlet at Head of Passes ($x = 0$; Figure 2). This condition effectively shuts down suspended sand transport, and limits bed form transport ($Q_s/w < 0.1$ m^2/h) so that there is little downstream transfer of bed materials between alluvial bars in the final $\sim$165 km of the river [*Nittrouer et al.*, 2011b]. During high-water discharge ($Q > 3 \times 10^4$ m^3/s), bed material transport in the final 165 km of the river increases 100-fold, and sand flux over alluvial bars is equally partitioned between both bed form and suspended flux [*Biedenharn and Thorne*, 1994; *Nittrouer et al.*, 2011b]. Tight bend segments of the lower river lack alluvial sand cover indicating that transfer of bed materials through these segments likely occurs by suspended load transport [*Nittrouer et al.*, 2011a].

[23] We focus the simulations on the lower 500 km of the river because this encompasses the backwater/drawdown zone under most conditions, and it is downstream of the managed diversion of the Mississippi flow into the Atchafalaya River ($x = 502$ km), which complicates modeling [*Harmar et al.*, 2005] (Figure 2). All lateral positions are distances along the river relative to Head of Passes ($x = 0$ km) where the Mississippi River bifurcates into three main branches, each of which persists for a relatively short distance ($\sim$20 km) downstream before river flow enters the

Figure 2. Plan view map of the lowermost Mississippi River (blue thick line), including Tarbert Landing (x = 493 km), Baton Rouge (x = 367 km), New Orleans (x = 165 km), and Head of Passes (x = 0 km).

open ocean (Figure 2). As discussed above, our simple depth averaged model cannot realistically account for channel bifurcations, and instead we treat this as a zone of net channel widening. For the simulations we assume that flow occurs within a single-thread channel and neglect overbank flooding for simplicity. This is a reasonable assumption for the Mississippi River, as the levees are sufficient to contain most high-discharge events.

[24] The model results are presented in sections 4.1 and 4.2. First in section 4.1, we present model simulations with assumptions of a constant channel bed slope, channel width, and friction factor. These approximations are used to illustrate the drawdown behavior in the simplest way possible that is consistent with the conceptual model of *Lane* [1957]. This is problematic for simulations of the Mississippi River, however. Perhaps most significant is that the river bed topography does not follow a constant slope, but instead transitions over the lower 200 km from downstream sloping to horizontal, and finally to an adverse grade near $x = 35$ km. Normal flow is not defined for flat or adversely sloping beds [*Chow*, 1959]. The river cross-sectional area also varies in the downstream direction within this same zone. Both the adverse bed slope and changing cross-sectional area may act to enhance or diminish erosion induced by water surface drawdown. Thus, in section 4.2, we relax the assumptions made in section 4.1 and use available topographic data to drive the model.

4.1. Constant Channel Slope and Width

[25] In this section, we assume a constant channel bed slope ($S_b = 4.5 \times 10^{-5}$), a constant depth-averaged channel width ($w = 533$ m) and top width ($B = 945$ m) upstream of the river mouth ($x > 0$), and a constant friction factor ($C_f = 2 \times 10^{-3}$ [*Wright and Parker*, 2004]). The channel geometries are the average values within the lower 500 km of the river as calculated from channel cross-section measurements surveyed in 1974–1975 by the U.S. Army Corps of Engineers (discussed in section 4.2). The model results are shown in Figures 3 and 4 for three different discharges ($Q = 6.2 \times 10^3$, 2.9×10^4, and 4.2×10^4 m^3/s), which correspond to the low-flow discharge of 1968 (which is a typical base flow), the 1964 peak annual flood with an annual flood recurrence interval of 1.9 years, and the peak annual flood of 1997 with a recurrence interval of 27 years (Figure 5). All discharges were measured at Tarbert Landing, $x = 492$ km, downstream of the Atchafalaya River diversion. For each set discharge, the model was run for the case of no lateral spreading ($\theta = 0°$) (Figure 3) and $\theta = 5$ degrees of spreading (Figure 4) downstream of Head of Passes ($x = 0$). As shown in section 4.1.2, the model results are relatively insensitive to the angle of spreading for angles larger than about $\theta = 1°$.

[26] The results show that backwater extends beyond the upstream boundary of the model domain at low flow (Figures 3a and 4a), creating a zone of flow deceleration (Figures 3b and 4b) and deposition (Figures 3c and 4d) as expected. There is a greater rate of deposition for regions with larger water surface concavity (i.e., $x = 500$ km). At low flow, the model results are insensitive to the degree of lateral spreading except for $x < 0$ where spreading induces deposition (Figure 4c). For cases with no lateral spreading, larger discharges push the backwater zone seaward (Figure 3a) and the resulting peak in deposition rate translates toward the river mouth (Figure 3c). The backwater zone renders the river depositional everywhere upstream of its mouth if lateral spreading of the plume is neglected.

[27] The model predictions are strikingly different for the moderate and high-discharge cases that allow lateral spreading of the plume for $x < 0$ (Figure 4). For the high-discharge case,

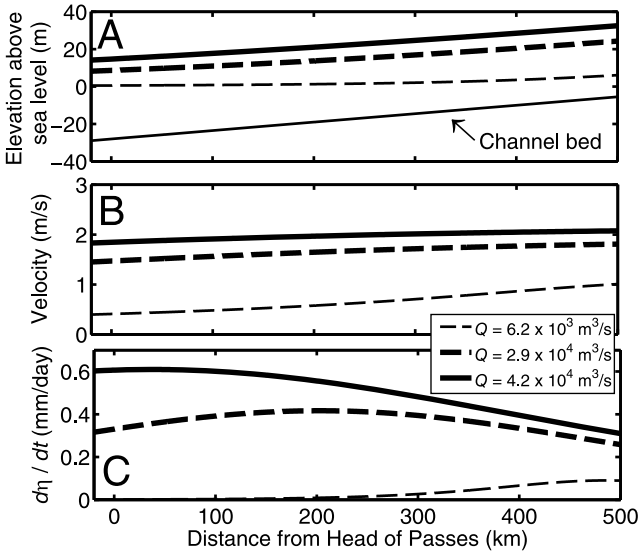

Figure 3. Model results of (a) water surface and bed elevations, (b) depth-averaged flow velocity, and (c) deposition rate for three discharge events on the Mississippi River as a function of upstream distance from Head of Passes. For each discharge event, model results are for the case without offshore plume spreading ($\theta = 0°$). Flow is from right to left.

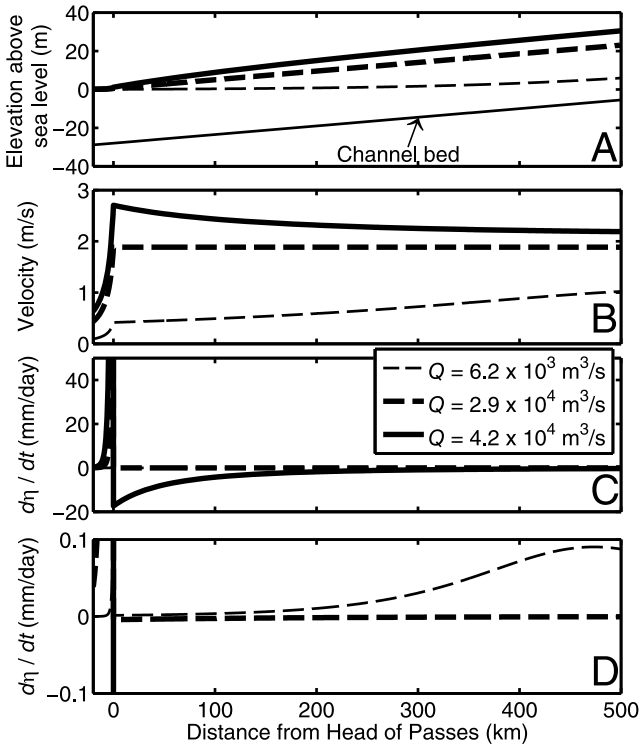

Figure 4. Model results of (a) water surface and bed elevations, (b) depth-averaged flow velocity, and (c and d) deposition rate for three discharge events on the Mississippi River as a function of upstream distance from Head of Passes. Figure 4d is a close-up of deposition rates in Figure 4c. For each discharge event, model results are shown for the case that allows spreading of the plume beyond the shoreline ($\theta = 5°$). Note that peak offshore deposition rate in Figure 4c is 170 and 1060 mm/d for $Q = 2.9 \times 10^4$ m^3/s and 4.2×10^4 m^3/s, respectively; the scale is set to better display erosion rates. Flow is from right to left.

spreading of the plume forces the elevation of the water surface at the shoreline to be very near sea level. In order for the fluvial water surface profile to match this elevation it forms a convex shape (Figure 4a) and flow *accelerates* toward the shoreline (Figure 4b) resulting in erosion of the riverbed (Figure 4c). The moderate flow scenario highlights an interesting transition point where normal flow conditions and sediment bypass can extend all the way to the shoreline. This special case marks the transition from backwater conditions at lesser water discharges to drawdown conditions at greater water discharges.

4.1.1. Comparison to Velocity Measurements

[28] We compare model results to 18 measurements of average flow velocity made by the U.S. Army Corps of Engineers at three locations (New Orleans, x = 165 km; Baton Rouge, x = 368 km; Red River Landing, x = 487 km) (Figure 6). These measurements were made at two-thirds the total depth to approximate the depth-averaged velocity and averaged across the channel width (G. E. Brown, U.S. Army Corps of Engineers, personal communication, 2010). The velocity data were reported as a function of stage height and discharge records are available only at Tarbert Landing (x = 492 km). To convert stage height to discharge, we fit a fourth-order polynomial to the log of discharge measured at x = 492 km and the log of stage height as measured at x = 165, 368, and 492 km. The best fit solutions to flow velocity versus discharge are shown in Figure 6, with the error bars representing plus and minus one geometric standard deviation. Interestingly, the measurements show a downstream deceleration of flow for low discharges and a downstream acceleration of flow at high discharges with the transition point occurring at about $Q = 3 \times 10^4$ m^3/s, which has a recurrence interval range of ~2 years (Figure 5), similar to the model results (Figure 4).

[29] A series of model solutions was calculated to compare to these measurements by systematically varying the discharge and noting the velocity at the three x locations where measurements were made (Figure 6). Although the match is imperfect, the model shows a transition from spatial deceleration to spatial acceleration at about $Q = 3 \times 10^4$ m^3/s. Note that the model simulations without spreading never produce this downstream reversal in velocity gradient; there is spatial deceleration for all discharge events for the simulations without spreading (Figure 3).

4.1.2. Effect of River Plume Spreading Angle

[30] To further explore model sensitivity, we performed a series of runs to evaluate the effect of river plume spreading angle on the water depth at the river mouth. These model runs follow the assumptions stated above for the Mississippi River using a constant channel slope, width, and bed friction. Results show that the water depth at the river mouth

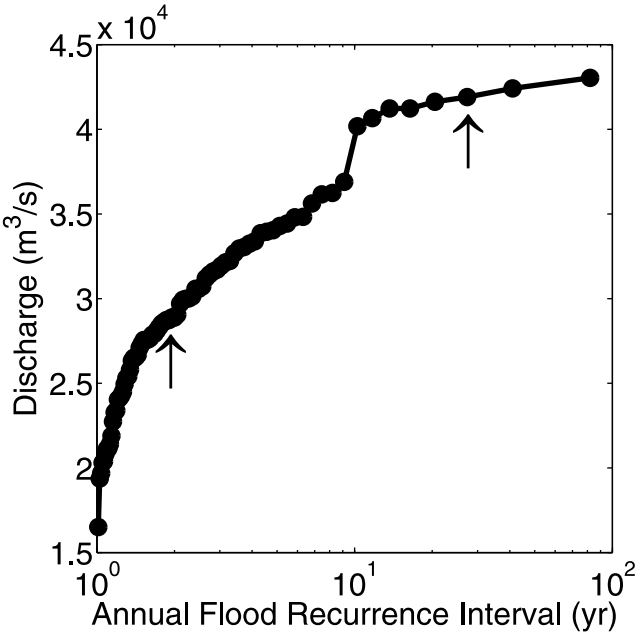

Figure 5. Recurrence interval calculated following the Weibull method for peak annual flood events on the Mississippi River as measured at Tarbert Landing, Mississippi (x = 492 km), from 1932 to 2010 (U.S. Army Corps of Engineers). The arrows point to the two flood discharges used in the model simulations ($Q = 2.9 \times 10^4$ and 4.2×10^4 m^3/s). Note that this record does not contain known earlier large floods, such as the great flood of 1927 with an estimated discharge at Tarbert Landing of 4.8×10^4 m^3/s (see text for details).

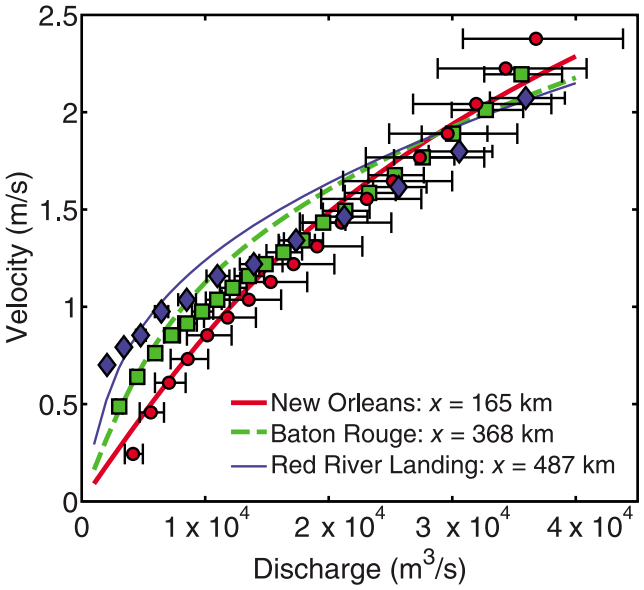

Figure 6. Model results for depth-averaged water velocities for a series of discharges at three locations: New Orleans (thick red line), Baton Rouge (dashed green line), and Red River Landing (thin blue line). For each station, model results are shown for the case that allows spreading of the plume beyond the shoreline (solid lines). Model results are compared to measurements of velocity by the U.S. Army Corps of Engineers at the three same stations (New Orleans (red circles), Baton Rouge (green squares), and Red River Landing (blue diamonds)). Error bars represent ±1 geometric standard deviation associated with the regression to convert stage height to discharge (see text for details).

varies little (<10%) from the no-flow depth (h_{nf}), that is the depth that would be due to ocean water inundation alone in the absence of river discharge (i.e., $Q = 0$), for spreading angles greater than about 1° (Figure 7). Under these conditions, the spreading of the plume is sufficient to hold the water surface elevation to very near sea level and river dynamics are not sensitive to the degree of spreading.

4.2. Full Channel Topography

[31] In order to simulate different flood events on the Mississippi River with more realistic bed topography, we imported measured river bed cross-sectional geometries surveyed in 1974–1975 by the U.S. Army Corps of Engineers. This data set includes cross sections spaced every 250 to 400 m along the river. The point spacing in each cross section varies, but is typically 30–40 m (e.g., see *Harmar and Clifford* [2007] for detailed analysis of the topographic data sets). To account for variations in river cross-sectional geometry, the topographic database was queried at each spatial node in the model to find the cross-sectional area of flow for a given water depth at a given streamwise location. Cross-sectional areas were linearly interpolated for model nodes that fell in between measured cross-section locations. The resultant bed topography shows considerable roughness resulting from bar-and-pool topography (Figure 8a). Because the model is depth averaged and the roughness is localized, it is necessary to average out much of the topographic variability before running the model, which was accomplished using a 100 km moving average window, which was linearly reduced with distance within $x < 100$ km due to the domain boundary (Figure 8a). Smaller window sizes do not change the overall results, but they do add significant noise.

[32] Unlike the simplified model in section 4.1, here we allow the coefficient of friction (C_f) to vary spatially as a result of changes in flow depth, form drag due to bed forms, Froude number, and the Shields stress. To accomplish this, we used the method of *Wright and Parker* [2004] to calculate the friction coefficient at each model node assuming a constant median sediment size of $D_{50} = 200$ microns [*United States Army Corps of Engineers*, 1935], $D_{90} = 3\ D_{50}$, and a flow stratification correction factor of $\alpha = 0.85$ [*Wright and Parker*, 2004]. This calculation was nested within the iterative scheme used in the backwater hydraulic calculation since C_f depends on the local velocity and depth.

[33] Model results are compared to stage heights measured at 19 to 21 stations and discharge measured at one station (Tarbert Landing, $x = 492$ km) managed by the U.S. Army Corps of Engineers. In order to correlate the stage heights to a given discharge, we assume that the minimum and maximum annual stage heights at each gage site correlated with the minimum and maximum annual discharge at $x = 492$ km. In addition to stage heights, we also compare the model results to measurements by the U.S. Army Corps of Engineers of flow velocities at three locations (New Orleans, $x =$ 165 km; Baton Rouge, $x = 368$ km; Red River Landing, $x =$ 492 km), which were introduced previously (i.e., Figure 6). Model results are shown for the same high, moderate and low discharges discussed in section 4.1. For the high-discharge case (the flood of 1997), the Bonnet Carre Spillway ($x = 206$ km) was opened allowing a peak outflow of 6.9×10^3 m^3/s reducing the peak discharge in the Mississippi River for $x < 206$ km from 4.2×10^4 m^3/s to 3.5×10^4 m^3/s. Our quasi-2-D model cannot properly incorporate a diversion,

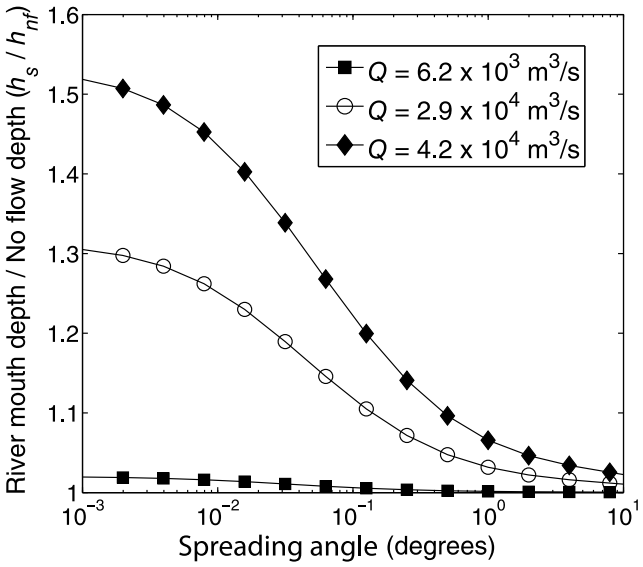

Figure 7. Model results for the case of the Mississippi River water depth at the river mouth normalized by the flow depth at the river mouth with no river discharge versus spreading angle of the offshore plume. Each point is a model run.

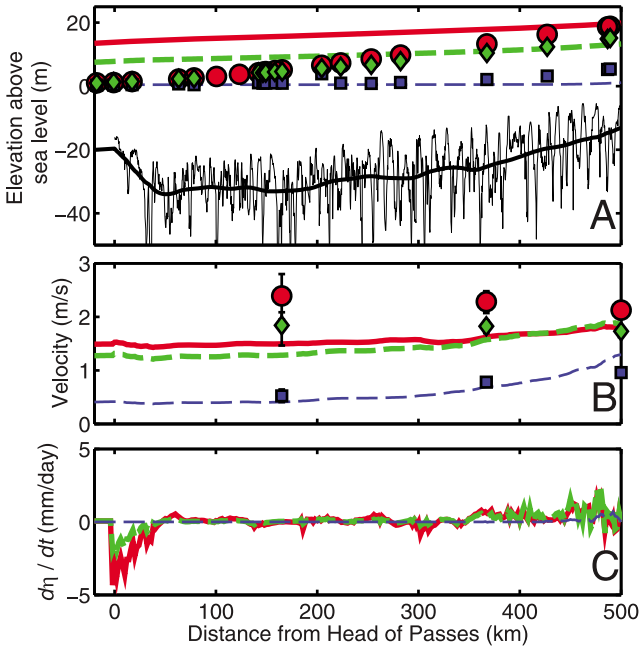

Figure 8. Model results of (a) water surface and bed elevations, (b) depth-averaged flow velocity, and (c) deposition rate for three discharge events on the Mississippi River as a function of distance from Head of Passes. For each discharge event, model results are shown for the case that does not allow spreading of the offshore plume ($\theta = 0°$). The results differ from those in Figure 3 because here we used measured bed topography (raw data and the smoothed thalweg profile are shown as thin and thick black lines, respectively, in Figure 8a), channel cross-sectional areas, and a model that allows spatially variable friction coefficients. Measured water surface elevations from 19 to 21 stations (Figure 8a) and water velocities from 3 stations (Figure 8b) are also shown (U.S. Army Corps of Engineers) for $Q = 4.2 \times 10^4$ m^3/s (red circles), $Q = 2.9 \times 10^4$ m^3/s (green diamonds), and $Q = 6.2 \times 10^3$ m^3/s (blue squares). Error bars in velocities represent ± 1 standard deviation from the fit between stage height and discharge (as in Figure 6). All stage heights are measured with respect to a single datum (NGVD29).

particularly for routing sediment; therefore, the model predictions for $x < 206$ km for this particular event may be taken as upper estimates. As in section 4.1, two different model scenarios are shown: one with no spreading where the width at $x < 0$ was set to the observed depth-averaged width at $x = 0$ km (i.e., $w = 520$ m) (Figure 8) and one with a constant rate of spreading of 5 degrees for $x < 0$ (Figure 9).

[34] As in section 4.1, model results for the case where the plume spreads (Figure 9a) match the observed stage heights better than the case without spreading (Figure 8a). Of particular importance is that the observed water surface elevations at $x = 0$ km are insensitive to discharge, which is consistent with the spreading model and inconsistent with the model without spreading. At low flow, both the model and the measured velocities show spatial deceleration (Figures 8b and 9b) which results in a small amount of deposition. In contrast, for the spreading case, high discharges produce spatial acceleration near the river mouth (Figure 9b) and erosion (Figures 9c and 9d). This is consistent with velocity measurements that also show spatial acceleration (Figure 9b). For the high-flow example shown, the modeled erosion rate into unconsolidated sediment is predicted to peak at $x = 10$ km at ~110 mm/d (Figure 9c) and scour persists upstream for ~170 km except for deposition from $60 < x < 80$ km and at ~120 km (Figure 9d). This length scale of scour is consistent with observations of eroding substrate in the lowermost Mississippi [*Nittrouer et al.*, 2011a]. However, actual erosion rates are likely less than these predictions where the alluvial mantle has been

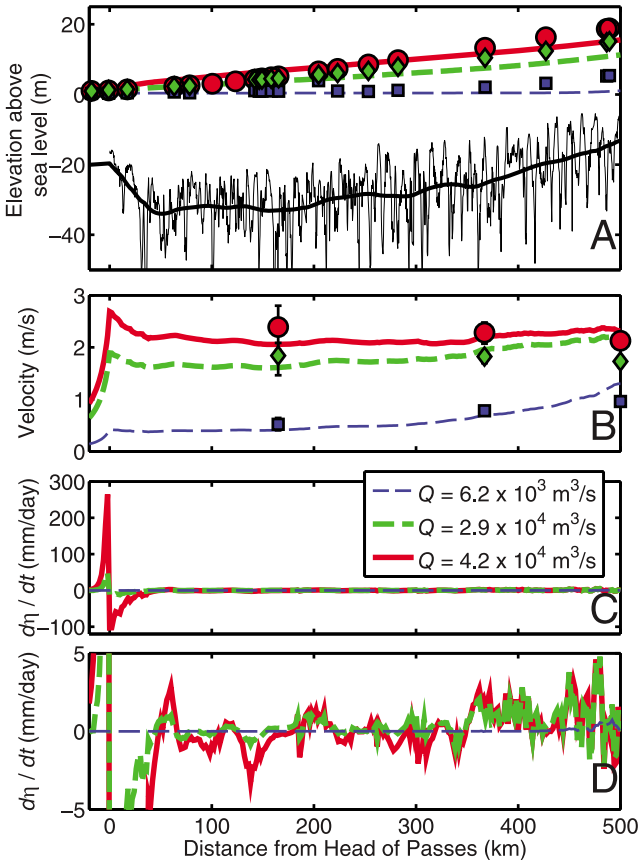

Figure 9. Model results of (a) water surface and bed elevations, (b) depth-averaged flow velocity, and (c and d) deposition rate for three discharge events on the Mississippi River as a function of distance from Head of Passes. Figure 9d is a close-up of deposition rates in Figure 9c. For each discharge event, model results are shown for the case that allows spreading of the offshore plume ($\theta = 5°$). The results differ from those in Figure 4 because here we used measured bed topography (raw data and the smoothed thalweg profile are shown as thin and thick black lines, respectively, in Figure 9a), channel cross-sectional areas, and a model that allows spatially variable friction coefficients. Measured water surface elevations from 19 to 21 stations (Figure 9a) and water velocities from three stations (Figure 9b) are also shown (U.S. Army Corps of Engineers) for $Q = 4.2 \times 10^4$ m^3/s (red circles), $Q = 2.9 \times 10^4$ m^3/s (green diamonds), and $Q = 6.2 \times 10^3$ m^3/s (blue squares). Error bars in velocities represent one standard deviation from the fit between stage height and discharge (as in Figure 6). All stage heights are measured with respect to a single datum (NGVD29).

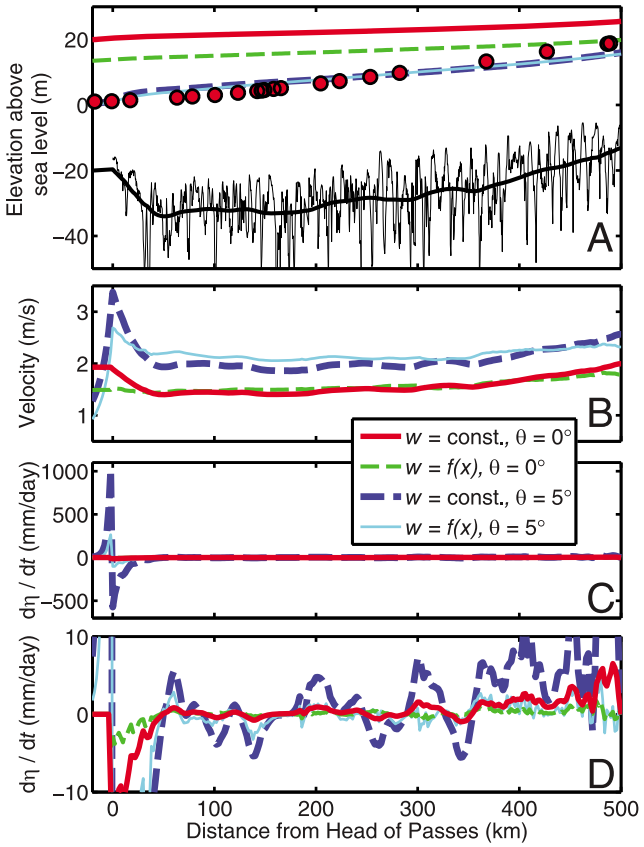

Figure 10. Model results of (a) water surface and bed elevations, (b) depth-averaged flow velocity, and (c and d) deposition rate for $Q = 4.2 \times 10^4$ m^3/s on the Mississippi River as a function of distance from Head of Passes. Figure 10d is a close-up of deposition rates in Figure 10c. The thin, solid light blue line shows the same model simulation as Figure 9 (i.e., variable channel width and a spreading plume with $\theta = 5°$). The thick, dark blue dashed line shows the model simulation with constant channel width (w = const.) and a spreading plume ($\theta = 5°$). The thick, solid red line shows the model simulation with a constant channel width (w = const.) and no spreading of the offshore plume ($\theta = 0°$). The thin, green dashed line shows the model simulation with variable channel width ($w = f(x)$) and no spreading of the offshore plume ($\theta = 0°$). Measured water surface elevations from 21 stations (Figure 10a) are also shown (U.S. Army Corps of Engineers).

stripped and erosion is occurring in the consolidated sediments below [*Nittrouer et al.*, 2011a]. The spreading model predicts a peak in deposition at $x = 0$ km resulting from spreading of the plume. This is consistent with a dramatic shallowing and bifurcations of channels in this region (Figure 9a).

[35] Unlike the simplified model runs in section 4.1 where drawdown was the only effect responsible for spatial acceleration and erosion, here, even without offshore plume spreading, there is acceleration and erosion in places due to adverse bed gradients (i.e., with an upstream oriented dip-slope direction) and spatial changes in channel width (Figure 8). Figure 10 shows model results for cases where we attempted to isolate these effects to see which are most important for inducing scour in the lower Mississippi River. The lower ~50 km of the Mississippi River has an adverse bed slope that likely is a result of the topographic rise associated with bifurcations, spreading, and deposition for $x < 0$. Independent of the drawdown effect, adverse bed slopes cause downstream flow acceleration in steady, gradually varied flow [*Chow*, 1959], which might lead to scour. Our model results show, however, that this is a minor effect for the case of the Mississippi River (Figure 10). The adverse bed slope enhances scour in the lower 50 km, but it alone is not the cause of erosion as predicted by the model. Model runs that include the adverse bed slope but do not allow offshore spreading of the plume show negligible scour as compared to those that allow spreading (Figure 10c).

[36] Like the adverse bed slope, downstream narrowing of the channel cross section might also induce flow acceleration and erosion. Indeed, downstream narrowing has been argued to be the potential cause of erosion in the lower Mississippi River [*Parker et al.*, 2009; *Nittrouer et al.*, 2012]. Although the channel top width decreases in the downstream direction between river kilometer 500 and 200, the top width increases in the downstream direction in the lower 200 km of the river (Figure 11). Moreover, the depth-averaged width is relatively constant within $80 < x < 400$ km and increases in the downstream direction within $0 < x < 80$ km (Figure 11). These width variations result in model simulations that predict less erosion near the river mouth when natural width variations are included in the model as compared to model runs where the width is held constant at the average value (Figure 10). Thus, downstream variations in channel width cannot explain scour near the river mouth.

5. Discussion

5.1. Simplified Criterion for Backwater/Drawdown Transition

[37] The control on whether backwater or drawdown will occur at the river mouth is a function of the normal-flow

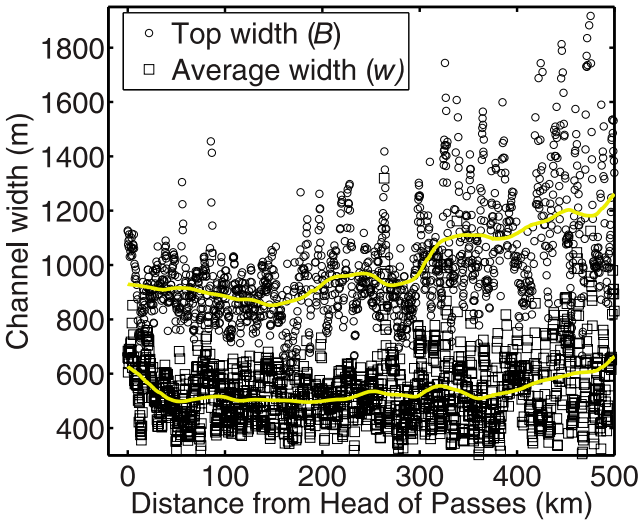

Figure 11. Measured top width (B) and depth-averaged width (w) at bankfull from cross sections as a function of distance upstream from Head of Passes. The solid lines are running averages using a 100 km smoothing window. Measurements are from the U.S. Army Corps of Engineers survey of 1974–1975.

depth (h_n) relative to the flow depth at the river mouth (h_s), where backwater (M1 curve) occurs for $h_n < h_s$, and drawdown (M2) occurs for $h_n > h_s$ [*Chow*, 1959]. The water depth at the river mouth is a function of river discharge as well as the dynamics of the offshore plume. However, as shown in section 4.1.2, only a small spreading angle (<1°) is needed to force the water surface elevation at the river mouth to be very near sea level. Since jet spreading angles tend to be >1° [*Wright and Coleman*, 1971; *Rajaratnam*, 1976; *Rowland et al.*, 2009; *Falcini and Jerolmack*, 2010], and observations of river mouth stage heights show little variation with respect to discharge [*Karadogan et al.*, 2009] (Figure 9a), it may be reasonable to assume that the water depth at the river mouth is equivalent to the no-flow water depth even during floods (i.e., $h_s \approx h_{nf}$). In such a case, the transition from M1 to M2 behavior can be found from a simple criterion by combining $h_n = h_s \approx h_{nf}$ with the definitions for normal flow $h_n = (C_f Q^2/gS_b w^2)^{1/3}$ and the Froude Number $F_{nf} = \left(\frac{Q^2}{gw^2 h_{nf}^3}\right)^{1/2}$ assuming a rectangular channel cross section (i.e., $B = w$), resulting in

$$F_{nf}{}^2 = \frac{S_b}{C_f}. \tag{4}$$

Given a coefficient of friction that is typical for alluvial rivers ($C_f = 5 \times 10^{-3}$ [*Parker et al.*, 2007]), it can be seen from inspection of equation (4) that a M2 drawdown curve is possible for rivers with subcritical flows ($F_{nf} < 1$) and small bed gradients ($S_b < 5 \times 10^{-3}$) that typify many coastal environments.

5.2. Backwater and Drawdown Length

[38] The distance upstream from the river mouth that is affected by backwater or drawdown (L) was found analytically for a rectangular channel by *Bresse* [1860],

$$\frac{LS_b}{h_n} = \varsigma_L - \varsigma_s + \left(1 - F^2\right)[Z(\varsigma_L) - Z(\varsigma_s)], \tag{5}$$

where ς is defined as the flow depth (h) divided by the normal depth (h_n). At the shoreline, $\varsigma = \varsigma_s = \frac{h_s}{h_n}$. Because the flow depth asymptotically approaches the normal flow depth in the upstream direction, $\varsigma = \varsigma_L$ is defined as the fractional depth where $x = L$. Herein, we set $\varsigma_L = 0.95$; that is, the upstream extent of backwater is defined as the location

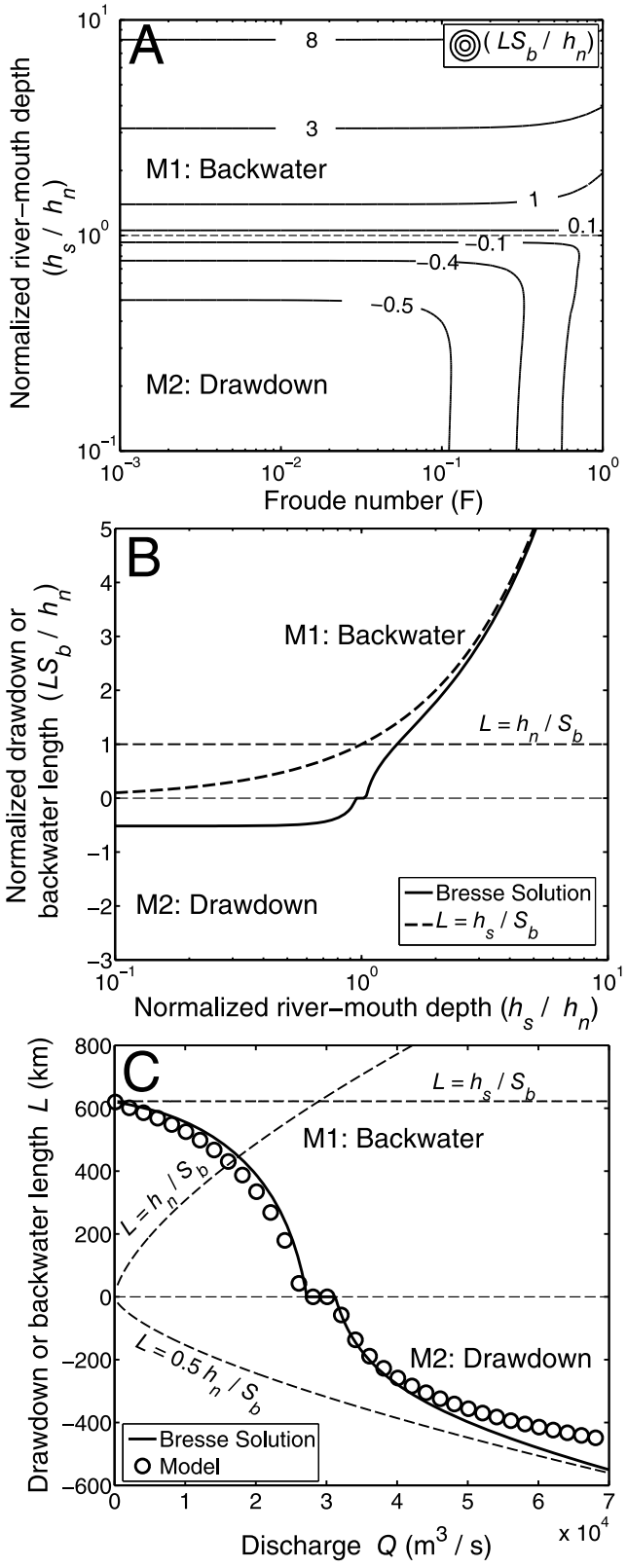

Figure 12. (a) Contours of the nondimensional backwater or drawdown length (i.e., LS_b/h_n) as calculated from equations (5) and (6) [*Bresse*, 1860] as a function of the water depth at the river mouth normalized by the normal flow depth and the Froude number. The drawdown length is set to be negative for visualization. The transition from backwater to drawdown is predicted at $h_s/h_n = 1$. (b) Nondimensional backwater or drawdown length versus normalized depth at the river mouth for the case of small Froude numbers (i.e., $F < 0.1$) as predicted by equations (5) and (6)) and by the scaling relationship $L = h_s/S_b$. (c) Modeled backwater or drawdown length as a function of discharge for the case of the Mississippi River. The symbols represent full model solutions, the solid line is equations (5) and (6), and dashed lines show proposed scaling relationships for the backwater length $L = h_s/S_b$ and $L = h_n/S_b$ and for the drawdown length $L = 0.5\, h_n/S_b$. The discontinuity in the model and solution by Bresse at $L = 0$ results from the threshold $\varsigma_L = 0.95$ used to define L.

where there is 5% deviation from the normal flow depth. $Z(\varsigma)$ is a function given by

$$Z(\varsigma) = \frac{1}{6}\ln\left(\frac{\varsigma^2+\varsigma+1}{(\varsigma-1)^2}\right) - \frac{1}{\sqrt{3}}\arctan\left(\frac{\sqrt{3}}{2\varsigma+1}\right). \quad (6)$$

The nondimensional length of backwater or drawdown (i.e., LS_b/h_n) given by equations (5) and (6) is a function of the Froude number and the relative depth at the shoreline ($\varsigma_s = \frac{h_s}{h_n}$) for a given value of ς_L. As shown in Figure 12a, LS_b/h_n has a maximum value of 0.5 for M2 conditions (we set L to be negative for M2 drawdown conditions for convenience), which occurs for small Froude numbers and small $\frac{h_s}{h_n}$. L tends to zero as $\frac{h_s}{h_n}$ or F approach unity. The backwater length can become arbitrarily large with increasing $\frac{h_s}{h_n}$ for $F < 1$ (Figure 12a).

[39] For $F < 0.1$, which is typical of large, low-gradient rivers, the solution to equation (5) is independent of F as the term $(1 - F^2) \rightarrow 1$ (Figure 12a). In this case, the nondimensional length scale is only a function of $\frac{h_s}{h_n}$ (Figure 12b). Backwater effects are often estimated by assuming $L \approx h_n/S_b$, which can be derived from a scaling analysis of the equations of momentum conservation [e.g., *Paola*, 2000]. This length scale does not characterize well the backwater length, but it does approximate twice the drawdown length for $\frac{h_s}{h_n} \ll 1$ (Figure 12b). An alternative length scale h_s/S_b characterizes well the backwater length for low-discharge M1 events when $\frac{h_s}{h_n} \gg 1$ (Figure 12b). However, it does not account for the reduction in L when $\frac{h_s}{h_n} \rightarrow 0$, $L = 0$ for $\frac{h_s}{h_n} = 1$, or the drawdown length scale for $\frac{h_s}{h_n} < 1$ (Figure 12b).

[40] These predictions indicate, for the case of the Mississippi River, that backwater lengths can extend ~600 km upstream during low flow, the transition from M1 to M2 occurs at about $Q = 3 \times 10^4$ m^3/s, and the drawdown length can extend up to ~200 km upstream during historical high flows (Figure 12c). This suggests that bypass and erosion in the lower Mississippi should be relatively common (flood recurrence intervals of 2 years or greater (Figure 5)), and that spatially extensive erosion likely has occurred in historical times. For example, a 7 year flood with a discharge of 3.5×10^4 m^3/s, has a predicted length scale of drawdown and erosion of ~150 km (Figure 12). This length scale of scour is consistent with observations of exposed and eroding substrate within the lower 160 km of the Mississippi River [*Nittrouer et al.*, 2012]. Note that the largest historical flood on the lower Mississippi River (1927) has been estimated to be $\sim 4.8 \times 10^4$ m^3/s [*Barry*, 1997], which has a predicted drawdown length of 340 km.

5.3. Effect of Levees and Overbank Flow

[41] Perhaps the most restrictive assumption we have made in the model is to assume no overbank flow over an extensive floodplain. This is a reasonable assumption for the Mississippi River, as the levees are capable of containing most high-discharge events [*Kesel et al.*, 1974]. To illustrate this, Figure 13 shows the average of the left and right bankfull elevations of the Mississippi River as extracted from the 1974–1975 by the U.S. Army Corps of Engineers channel cross-section data. Like the cross sections discussed above, the levee elevations were smoothed using a 100 km moving average filter. Note that in many places within the lower Mississippi River valley there exist man-made secondary levees that are set back from the natural channel edge by less than 100 m (but in cases extending ~1 km from the natural channel edge). The elevations of these secondary levees (as measured in Google Earth) are meters higher than the bankfull elevations (Figure 13). From these measurements, it is clear that large flood events with modeled discharges up to $\sim Q = 4 \times 10^4$ m^3/s, which is well within the drawdown regime, would be contained by the secondary levees.

[42] The effect of a coupled floodplain on drawdown dynamics likely depends on the nature of floods in a particular river system. For example, flow from the channel to the floodplain would reduce the rate of water surface elevation rise in the channel, which in turn could reduce the magnitude of drawdown and scour, at least until the floodplain is fully inundated. However, in some rivers (including reaches of the Mississippi), water levels can rise contemporaneously in the floodplain and channel, or water can flow from the floodplain to the channel due to floodplain inundation from upstream sources or direct precipitation [e.g., *Mertes*, 1997; *Day et al.*, 2008]. In these cases, the floodplain may have little effect on drawdown and scour.

5.4. Implications for Channel Dynamics

[43] The characteristic discharge hypothesis is one of the most important in fluvial morphodynamics. It poses that

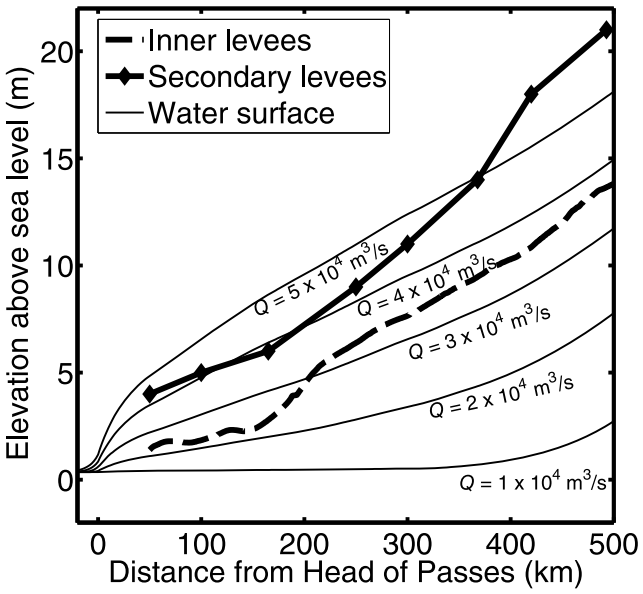

Figure 13. Measured levee and modeled water surface elevations as a function of distance from Head of Passes. The bankfull levee heights were measured as the average of the left and right bankfull elevations of the Mississippi River as extracted from the 1974–1975 by the U.S. Army Corps of Engineers channel cross-section data and smoothed with a 100 km moving average filter. The secondary levees were measured using Google Earth. Water surface elevations for a range of discharges are from model simulations that include the full channel topography and a spreading angle of 5°.

subject to a range of river discharge events, self-formed river channels adjust to an equilibrium state where a single characteristic or bankfull discharge dominates channel form and sediment transport over geomorphic timescales [*Wolman and Miller*, 1960]. The hypothesis is the foundation of models of fluvial morphodynamics [*Paola et al.*, 1992; *Swenson and Muto*, 2007] and drainage basin evolution [*Tucker and Slingerland*, 1997; *Fagherazzi et al.*, 2004] because it indicates that, despite a complex history of river flood events, channel dynamics can be understood by considering only a single characteristic discharge. Although the characteristic discharge hypothesis is supported by field data in alluvial rivers far upstream of the river mouth [*Williams*, 1978; *Parker et al.*, 2007], it has been questioned in bedrock rivers [*Tucker*, 2004; *Lague et al.*, 2005], and it is unclear if it holds in the backwater zone where flows are nonuniform, and the magnitude and extent of spatial deceleration/acceleration are sensitive to river discharge and river mouth boundary conditions.

[44] Our model of the lower Mississippi River indicates that the channel is near bankfull at $Q = 3 \times 10^4$ m^3/s (Figure 13). This result is similar to the work of *Biedenharn and Thorne* [1994] that showed that $Q = 3 \times 10^4$ m^3/s is the dominant discharge in the lower Mississippi River in terms of the maximum sediment transport work. Moreover, $Q = 3 \times 10^4$ m^3/s has a recurrence interval of ~2 years (Figure 5), which is very similar to that observed in rivers far upstream of backwater dynamics [*Williams*, 1978; *Parker et al.*, 2007]. Furthermore, at $Q = 3 \times 10^4$ m^3/s the model predicts a fundamental hydrodynamic transition from M1 backwater to M2 drawdown behavior and a morphodynamic transition from net deposition at lower flows to net erosion at higher flows (Figures 4, 6, 9, and 12). These results suggest that the river channel morphology may be adjusted to a discharge where the flow is uniform and sediment can bypass the lower river.

[45] This notwithstanding, it is not clear whether source-to-sink sediment transport and fluvial morphodynamics can be modeled using the characteristic discharge concept. With a single discharge, stable sea level and in the absence of delta progradation, models for river morphodynamics evolve to normal flow conditions everywhere (e.g., G. Parker, online book, 2004). Our model results suggest, on the other hand, that it is transient adjustment of the river to low-flow and high-flow events that allows a persistent backwater/drawdown zone. This zone in turn act as a filter on sediment transfer to marine environments whereby sediment flux from low-discharge events is muted and sediment flux from high-discharge events is enhanced from what would be expected from normal flow alone.

[46] Drawdown and scour in the lower reaches of coastal rivers may have implications for planform channel dynamics. It has been hypothesized that backwater dynamics might be responsible for the reduction in sinuosity seen in the lower portions of coastal rivers [*Harmar and Clifford*, 2006; *Jerolmack*, 2009; *Parker et al.*, 2009; *Nittrouer et al.*, 2012]. For example, sinuosity is significantly less in the lower ~300 km of the Mississippi River than farther upstream (Figure 2). *Hudson and Kesel* [2000] employed historic survey records to reconstruct channel migration rates on the Mississippi River and found migration rates locally exceeded 120 m/yr between 1877 and 1924 for $x > 500$ km and dropped to less than 10 m/yr in the lower 300 river kilometers. *Jerolmack and Mohrig* [2007] noted that deltaic distributary channels in general tend to have very small rates of lateral migration. Lateral channel migration is driven in part by bar growth [e.g., *Ikeda et al.*, 1981; *Parker et al.*, 2011], and bars have been observed to be lacking or degraded in the lower Mississippi River [*Nittrouer et al.*, 2012]. Thus, the potential for sediment bypass and erosion in the lower portion of coastal rivers during high flows offers a potential explanation for degraded bars and reduced sinuosity.

5.5. Implications for River Plume Dynamics

[47] Backwater dynamics are expected to have an important influence on river plume behavior and sedimentation. For example, backwater dynamics might serve to charge river plumes with sediment during large magnitude floods, increasing the density of the flow and encouraging hyperpycnal plunging plumes [*Mulder and Syvitski*, 1995]. There also exists the potential for dynamic feedback between backwater flow and the offshore river plume. For example, although it is well known that the dynamics and sedimentation patterns of offshore river plumes are strongly affected by discharge and sediment concentration of the feeder river [*Bates*, 1953; *Rajaratnam*, 1976; *Wright*, 1977; *Geyer et al.*, 2004; *Edmonds and Slingerland*, 2008; *Rowland et al.*, 2009; *Falcini and Jerolmack*, 2010; *Lamb et al.*, 2010], little work has explored whether river dynamics and sediment flux in turn are a function of plume behavior. Our modeling results suggest that the angle of plume spreading can affect the flow velocity and sediment concentration in the river, at least for small spreading angles.

5.6. Implications for Delta Morphodynamics

[48] The evolution of deltas is often modeled using steady flow equations and a single characteristic discharge [*Flemings and Jordan*, 1989; *Paola et al.*, 1992; *Swenson et al.*, 2005; *Edmonds and Slingerland*, 2007, 2008]. However, some workers have linked backwater hydrodynamics with changes in the patterns of deposition, which may in turn control the frequency of river avulsions and the length scale of delta lobes [e.g., *Hoyal and Sheets*, 2009; *Jerolmack*, 2009; *Chatanantavet et al.*, 2012]. Channel bifurcations, like unconfined plumes, can result in a net increase in channel width [e.g., *Edmonds and Slingerland*, 2007; *Shaw and Mohrig*, 2009], and therefore may induce enough spreading to cause drawdown at high flow. The result would be a trunk channel that scours upstream of the bifurcation and deposits downstream. There is evidence for such behavior in the morphology of bifurcations that show a deepening toward the bifurcation and a dramatic shallowing at the bifurcation. For example, *Roberts et al.* [1980] claimed that the large flood of 1973 in the Atchafalaya delta basin was responsible for significant erosion in the Atchafalaya basin which led to the initiation of both the Atchafalaya and Wax Lake deltas. Results from 3-D morphodynamic simulations of *Edmonds and Slingerland* [2007] also show scour, in some cases, upstream of an evolving bifurcation; however, the potential for M2 hydrodynamics was not addressed in their study. Once a delta has formed, erosion and deposition in distributary channels regulates the rate at which spreading can occur, and it is possible that these channels evolve in tandem with the

backwater flow dynamics. For example, *Kim et al.* [2009] linked elongate deltas like the Mississippi River to those that are able to maintain a spatially persistent and stable trunk channel, and scour during drawdown conditions would help to establish such a conduit.

[49] Over longer timescales, the case has been made that a river will always aggrade when propagating a delta into a basin with constant sea level [e.g., *Muto and Swenson*, 2006]. This occurs because as the delta progrades, the river must aggrade to maintain a sufficient bed slope to transport sediment across the delta topset. These ideas are in contrast to classic models of rivers reaching a dynamic equilibrium (i.e., grade) during periods of stable sea level [*Davis*, 1902]. Our modeling suggests that some rivers can scour their beds at high flows due to drawdown dynamics. This is because river hydraulics is a function of the water surface slope in addition to bed slope, and the two can diverge near river mouths. Thus, drawdown allows for the possibility of grade or even degradation during progradation (with a stable sea level) depending on the length of backwater in comparison to the size of the delta [cf. *Edmonds et al.*, 2011]. This notwithstanding, deltas are net depositional landforms and channel morphology must evolve so that bed erosion events do not dominate patterns in mass flux over geomorphic timescales. These scour events, however, likely leave unconformities in fluvio-deltaic stratigraphy, which may appear similar to those previously interpreted to be a result of relative sea level changes or other allogenic forcings [e.g., *Galloway*, 1989; *Posamentier et al.*, 1992; *Blum and Törnqvist*, 2000; *Paola*, 2000].

6. Conclusions

[50] Rivers are often assumed to decelerate and deposit sediment near their mouths due to a zone of backwater. We use a quasi-2-D hydrodynamic and sediment transport model to show that the transitional region that connects upstream normal river flow to the offshore river plume also can be a zone of erosion. This occurs at high discharges when the water depth at the river mouth is less than the normal flow water depth, which draws the water surface down creating flow acceleration. Drawdown ultimately occurs because spreading of the offshore plume forces the water surface elevation at the river mouth to be relatively insensitive to changes in discharge. Model results, and stage heights and velocities measured in the lower 500 km of the Mississippi River, suggest that the lower river experiences erosion for flood events with a recurrence interval larger than ~2 years. More frequent, smaller discharge floods have a backwater zone that can act as a filter forcing deposition, retarding source-to-sink sediment transfer. Large flood events with divergent offshore plumes, however, can eliminate the backwater zone resulting in fluvial erosion and enhanced sediment delivery basinward. The zones of erosion and deposition are predicted to have extended for hundreds of kilometers upstream of the river mouth for historic flood events. Coupled models of river and river plume systems driven by a suite of discharges may be needed to accurately capture sediment-transport dynamics of fluvio-deltaic systems.

[51] **Acknowledgments.** We thank O. P. Harmar for providing access to digital Mississippi River topographic data, and we thank the U.S. Army Corps of Engineers for providing access to measurement databases. Acknowledgment is made to the Donors of the American Chemical Society Petroleum Research Fund (grant to M.P.L.), the RioMAR Industry Consortium, and the National Science Foundation (grant EAR0948224 to J.A.N.). We thank Chris Paola, Federico Falcini, Dimitri Lague, and Alexander Densmore for their constructive reviews.

References

Allen, J. R. L. (1971), Transverse erosional marks of mud and rock: Their physical basis and geological significance, *Sediment. Geol.*, *5*(3–4), 167–385, doi:10.1016/0037-0738(71)90001-7.

Anderson, J. B., and A. B. Rodriguez (Eds.) (2008), *Response of Upper Gulf Coast Estuaries to Holocene Climate Change and Sea-Level Rise*, 146 pp., Geol. Soc. of Am., Boulder, Colo.

Barry, J. M. (1997), *Rising Tide*, 574 pp., Simon and Schuster, New York.

Bates, C. C. (1953), Rational theory of delta formation, *Am. Assoc. Pet. Geol. Bull.*, *37*(9), 2119–2162.

Biedenharn, D. S., and C. R. Thorne (1994), Magnitude frequency-analysis of sediment transport in the lower Mississippi River, *Reg. Rivers Res. Manage.*, *9*(4), 237–251, doi:10.1002/rrr.3450090405.

Blum, M. D., and T. E. Törnqvist (2000), Fluvial responses to climate and sea-level change: A review and look forward, *Sedimentology*, *47*, 2–48, doi:10.1046/j.1365-3091.2000.00008.x.

Bresse, J. A. C. (1860), *Cours de Mecanique Appliquee, Hydraulique*, 2nd ed., Mallet-Bachelier, Paris.

Carey, W. C., and M. D. Keller (1957), Systematic changes in the beds of alluvial rivers, *Proc. Am. Soc. Civ. Eng.*, *83*(1331), 1–24.

Chang, H. H. (1982), Fluvial hydraulics of deltas and alluvial fans, *J. Hydraul. Div. Am. Soc. Civ. Eng.*, *108*(11), 1282–1295.

Chatanantavet, P., M. P. Lamb, and J. A. Nittrouer (2012), Backwater controls on avulsion location on deltas, *Geophys. Res. Lett.*, doi:10.1029/2011GL050197, in press.

Chow, V. T. (1959), *Open-Channel Hydraulics*, 680 pp., McGraw-Hill, New York.

Davis, W. M. (1902), Baselevel, grade and peneplain, *J. Geol.*, *10*, 77–111, doi:10.1086/620982.

Day, G., W. E. Dietrich, J. C. Rowland, and A. Marshall (2008), The depositional web on the floodplain of the Fly River, Papua New Guinea, *J. Geophys. Res.*, *113*, F01S02, doi:10.1029/2006JF000622.

Edmonds, D. A., and R. L. Slingerland (2007), Mechanics of river mouth bar formation: Implications for the morphodynamics of delta distributary networks, *J. Geophys. Res.*, *112*, F02034, doi:10.1029/2006JF000574.

Edmonds, D. A., and R. L. Slingerland (2008), Stability of delta distributary networks and their bifurcations, *Water Resour. Res.*, *44*, W09426, doi:10.1029/2008WR006992.

Edmonds, D. A., J. B. Shaw, and D. Mohrig (2011), Topset-dominated deltas: A new model for river delta stratigraphy, *Geology*, *39*(12), 1175–1178, doi:10.1130/G32358.1.

Engelund, F., and E. Hansen (1967), *A Monograph on Sediment Transport in Alluvial Streams*, Teknisk Forlag, Copenhagen.

Fagherazzi, S., A. D. Howard, and P. L. Wiberg (2004), Modeling fluvial erosion and deposition on continental shelves during sea level cycles, *J. Geophys. Res.*, *109*, F03010, doi:10.1029/2003JF000091.

Falcini, F., and D. J. Jerolmack (2010), A potential vorticity theory for the formation of elongate channels in river deltas and lakes, *J. Geophys. Res.*, *115*, F04038, doi:10.1029/2010JF001802.

Flemings, P. B., and T. E. Jordan (1989), A synthetic stratigraphic model of foreland basin development, *J. Geophys. Res.*, *94*, 3851–3866, doi:10.1029/JB094iB04p03851.

Fong, D. A., and W. R. Geyer (2002), The alongshore transport of freshwater in a surface-trapped river plume, *J. Phys. Oceanogr.*, *32*(3), 957–972, doi:10.1175/1520-0485(2002)032<0957:TATOFI>2.0.CO;2.

Galler, J. J., T. S. Bianchi, M. A. Allison, L. A. Wysocki, and R. Campanella (2003), Biogeochemical implications of levee confinement in the lowermost Mississippi River, *Eos Trans. AGU*, *84*(44), 469, doi:10.1029/2003EO440001.

Galloway, W. E. (1989), Genetic stratigraphic sequences in basin analysis I: Architecture and genesis of flooding-surface bounded depositional units, *AAPG Bull.*, *73*(2), 125–142.

Geyer, W. R., P. S. Hill, and G. C. Kineke (2004), The transport, transformation and dispersal of sediment by buoyant coastal flows, *Cont. Shelf Res.*, *24*(7–8), 927–949, doi:10.1016/j.csr.2004.02.006.

Harmar, O. P., and N. J. Clifford (2006), Planform dynamics of the lower Mississippi River, *Earth Surf. Processes Landforms*, *31*(7), 825–843, doi:10.1002/esp.1294.

Harmar, O. P., and N. J. Clifford (2007), Geomorphological explanation of the long profile of the lower Mississippi River, *Geomorphology*, *84*(3–4), 222–240, doi:10.1016/j.geomorph.2006.01.045.

Harmar, O. P., N. J. Clifford, C. R. Thorne, and D. S. Biedenharn (2005), Morphological changes of the lower Mississippi River: Geomorphological response to engineering intervention, *River Res. Appl.*, *21*(10), 1107–1131, doi:10.1002/rra.887.

Horner-Devine, A. R. (2009), The bulge circulation in the Columbia River plume, *Cont. Shelf Res.*, *29*(1), 234–251, doi:10.1016/j.csr.2007.12.012.

Horner-Devine, A. R., D. A. Fong, S. G. Monismith, and T. Maxworthy (2006), Laboratory experiments simulating a coastal river inflow, *J. Fluid Mech.*, *555*, 203–232, doi:10.1017/S0022112006008937.

Hotchkiss, R. H., and G. Parker (1991), Shock fitting of aggradational profiles due to backwater, *J. Hydraul. Eng.*, *117*(9), 1129–1144, doi:10.1061/(ASCE)0733-9429(1991)117:9(1129).

Hoyal, D. C. J. D., and B. A. Sheets (2009), Morphodynamic evolution of experimental cohesive deltas, *J. Geophys. Res.*, *114*, F02009, doi:10.1029/2007JF000882.

Hudson, P. F., and R. H. Kesel (2000), Channel migration and meander-bend curvature in the lower Mississippi River prior to major human modification, *Geology*, *28*, 531–534, doi:10.1130/0091-7613(2000)28<531:CMAMCI>2.0.CO;2.

Ikeda, S., G. Parker, and K. Sawai (1981), Bend theory of river meanders. Part 1. Linear development, *J. Fluid Mech.*, *112*, 363–377, doi:10.1017/S0022112081000451.

Jerolmack, D. J. (2009), Conceptual framework for assessing the response of delta channel networks to Holocene sea level rise, *Quat. Sci. Rev.*, *28*(17–18), 1786–1800, doi:10.1016/j.quascirev.2009.02.015.

Jerolmack, D. J., and D. Mohrig (2007), Conditions for branching in depositional rivers, *Geology*, *35*, 463–466, doi:10.1130/G23308A.1.

Karadogan, E., C. S. Willson, and C. R. Berger (2009), Numerical modeling of the lower Mississippi River—Influence of forcings on flow distribution and impact of sea level rise on the system, in *OCEANS, Marine Technology for Our Future: Global and Local Challenges*, pp. 1–7, Mar. Technol. Soc., Biloxi, Miss.

Kesel, R. H., K. C. Dunne, R. C. McDonald, K. R. Allison, and B. E. Spicer (1974), Lateral erosion and overbank deposition on the Mississippi River in Louisiana caused by 1973 flooding, *Geology*, *2*, 461–464, doi:10.1130/0091-7613(1974)2<LEAODO>2.0.CO;2.

Kim, W., A. Dai, T. Muto, and G. Parker (2009), Delta progradation driven by an advancing sediment source: Coupled theory and experiment describing the evolution of elongated deltas, *Water Resour. Res.*, *45*, W06428, doi:10.1029/2008WR007382.

Kourafalou, V. H., L.-Y. Oey, J. D. Wang, and T. N. Lee (1996), The fate of river discharge on the continental shelf: 1. Modeling the river plume and the inner shelf coastal current, *J. Geophys. Res.*, *101*, 3415–3434, doi:10.1029/95JC03024.

Lague, D., N. Hovius, and P. Davy (2005), Discharge, discharge variability, and the bedrock channel profile, *J. Geophys. Res.*, *110*, F04006, doi:10.1029/2004JF000259.

Lamb, M. P., and D. Mohrig (2009), Do hyperpycnal-plume deposits record river-flood dynamics?, *Geology*, *37*, 1067–1070, doi:10.1130/G30286A.1.

Lamb, M. P., P. M. Myrow, C. Lukens, K. Houck, and J. Strauss (2008), Deposits from wave-influenced turbidity currents: Pennsylvanian Minturn Formation, Colorado, U.S.A., *J. Sediment. Res.*, *78*(7), 480–498, doi:10.2110/jsr.2008.052.

Lamb, M. P., B. McElroy, B. Kopriva, J. Shaw, and D. Mohrig (2010), Linking river-flood dynamics to hyperpycnal-plume deposits: Experiments, theory, and geological implications, *Geol. Soc. Am. Bull.*, *122*(9–10), 1389–1400, doi:10.1130/B30125.1.

Lane, E. W. (1957), *A Study of the Shape of Channels Formed by Natural Streams Flowing in Erodible Material*, U.S. Army Corps of Eng., Mo. River Div., Omaha, Nebr.

Mattheus, C. R., A. B. Rodriguez, D. L. Greene Jr., A. R. Simms, and J. B. Anderson (2007), Control of upstream variables on incised-valley dimension, *J. Sediment. Res.*, *77*(3), 213–224, doi:10.2110/jsr.2007.022.

McCabe, R. M., P. MacCready, and B. M. Hickey (2009), Ebb-tide dynamics and spreading of a large river plume, *J. Phys. Oceanogr.*, *39*(11), 2839–2856, doi:10.1175/2009JPO4061.1.

Mertes, L. A. K. (1997), Documentation and significance of the perirheic zone on inundated floodplains, *Water Resour. Res.*, *33*, 1749–1762, doi:10.1029/97WR00658.

Mulder, T., and J. P. M. Syvitski (1995), Turbidity currents generated at river mouths during exceptional discharges to the world oceans, *J. Geol.*, *103*, 285–299, doi:10.1086/629747.

Muto, T. (2001), Shoreline autoretreat substantiated in flume experiments, *J. Sediment. Res.*, *71*(2), 246–254, doi:10.1306/091400710246.

Muto, T., and J. B. Swenson (2006), Autogenic attainment of large-scale alluvial grade with steady sea-level fall: An analog tank-flume experiment, *Geology*, *34*, 161–164, doi:10.1130/G21923.1.

Nittrouer, C. A. (1999), STRATAFORM: Overview of its design and synthesis of its results, *Mar. Geol.*, *154*(1–4), 3–12, doi:10.1016/S0025-3227(98)00128-5.

Nittrouer, J. A., D. Mohrig, M. A. Allison, and A. B. Peyret (2011a), The lowermost Mississippi River: A mixed bedrock-alluvial, *Sedimentology*, doi:10.1111/j.1365-3091.2011.01245.x, in press.

Nittrouer, J. A., D. Mohrig, and M. A. Allison (2011b), Punctuated sand transport in the lowermost Mississippi River, *J. Geophys. Res.*, *116*, F04025, doi:10.1029/2011JF002026.

Nittrouer, J. A., J. Shaw, M. P. Lamb, and D. Mohrig (2012), Spatial and temporal trends for water-flow velocity and bed-material transport in the lower Mississippi River, *Geol. Soc. Am. Bull.*, doi:10.1130/B30497.1, in press.

Paola, C. (2000), Quantitative models of sedimentary basin filling, *Sedimentology*, *47*, 121–178, doi:10.1046/j.1365-3091.2000.00006.x.

Paola, C., P. L. Heller, and C. L. Angevine (1992), The large scale dynamics of grain-size variation in alluvial basins, 1: Theory, *Basin Res.*, *4*, 73–90, doi:10.1111/j.1365-2117.1992.tb00145.x.

Paola, C., R. R. Twilley, D. A. Edmonds, W. Kim, D. Mohrig, G. Parker, E. Viparelli, and V. R. Voller (2011), Natural processes in delta restoration: Application to the Mississippi Delta, *Annu. Rev. Mater. Sci.*, *3*, 67–91, doi:10.1146/annurev-marine-120709-142856.

Parker, G., P. R. Wilcock, C. Paola, W. E. Dietrich, and J. Pitlick (2007), Physical basis for quasi-universal relations describing bankfull hydraulic geometry of single-thread gravel bed rivers, *J. Geophys. Res.*, *112*, F04005, doi:10.1029/2006JF000549.

Parker, G., T. Muto, Y. Akamatsu, W. E. Dietrich, and J. W. Lauer (2008a), Unravelling the conundrum of river response to rising sea-level from laboratory to field. Part II: The Fly–Strickland River system, Papua New Guinea, *Sedimentology*, *55*, 1657–1686, doi:10.1111/j.1365-3091.2008.00962.x.

Parker, G., T. Muto, Y. Akamatsu, W. E. Dietrich, and J. W. Lauer (2008b), Unravelling the conundrum of river response to rising sea-level from laboratory to field. Part I: Laboratory experiments, *Sedimentology*, *55*, 1643–1655, doi:10.1111/j.1365-3091.2008.00961.x.

Parker, G., J. A. Nittrouer, D. C. Mohrig, M. A. Allison, W. E. Dietrich, and V. R. Voller (2009), Modeling the morphodynamics of the lower Mississippi River as a quasi-bedrock river, *Eos Trans. AGU*, *90*(52), Fall Meet. Suppl., Abstract EP32A-01.

Parker, G., Y. Shimizu, G. V. Wilkerson, E. C. Eke, J. D. Abad, J. W. Lauer, C. Paola, W. E. Dietrich, and V. R. Voller (2011), A new framework for modeling the migration of meandering rivers, *Earth Surf. Processes Landforms*, *36*(1), 70–86, doi:10.1002/esp.2113.

Posamentier, H. W., G. P. Allen, D. P. James, and M. Tesson (1992), Forced regressions in a sequence stratigraphic framework—Concepts, examples, and exploration significance, *AAPG Bull.*, *76*(11), 1687–1709.

Rajaratnam, N. (1976), *Turbulent Jets*, 302 pp., Elsevier, New York.

Roberts, H. H., R. D. Adams, and R. H. W. Cunningham (1980), Evolution of sand-dominant subaerial phase, Atchafalaya delta, Louisiana, *AAPG Bull.*, *64*(2), 264–279.

Rowland, J. C., M. T. Stacey, and W. E. Dietrich (2009), Turbulent characteristics of a shallow wall-bounded plane jet: Experimental implications for river mouth hydrodynamics, *J. Fluid Mech.*, *627*, 423–449, doi:10.1017/S0022112009006107.

Rowland, J. C., W. E. Dietrich, and M. T. Stacey (2010), Morphodynamics of subaqueous levee formation: Insights into river mouth morphologies arising from experiments, *J. Geophys. Res.*, *115*, F04007, doi:10.1029/2010JF001684.

Schiller, R. V., and V. H. Kourafalou (2010), Modeling river plume dynamics with the Hybrid Coordinate Ocean Model, *Ocean Modell.*, *33*(1–2), 101–117, doi:10.1016/j.ocemod.2009.12.005.

Schiller, R. V., V. H. Kourafalou, P. Hogan, and N. D. Walker (2011), The dynamics of the Mississippi River plume: Impact of topography, wind and offshore forcing on the fate of plume waters, *J. Geophys. Res.*, *116*, C06029, doi:10.1029/2010JC006883.

Shaw, J. B., and D. C. Mohrig (2009), Incised bifurcations and uneven radial distribution of channel incision in the Wax Lake Delta, USA, *Eos. Trans. AGU*, *90*(52), Fall Meet. Suppl., Abstract EP41A-0593.

Sheets, B. A., T. A. Hickson, and C. Paola (2002), Assembling the stratigraphic record: Depositional patterns and time-scales in an experimental alluvial basin, *Basin Res.*, *14*, 287–301, doi:10.1046/j.1365-2117.2002.00185.x.

Slingerland, R., J. W. Harbaugh, and K. Furlong (1994), *Simulating Clastic Sedimentary Basins*, Prentice Hall, Englewood Cliffs, N. J.

Snow, R. S., and R. L. Slingerland (1987), Mathematical modeling of graded river profiles, *J. Geol.*, *95*, 15–33, doi:10.1086/629104.

Swenson, J. B., and T. Muto (2007), Response of coastal plain rivers to falling relative sea-level: Allogenic controls on the aggradational phase, *Sedimentology*, *54*, 207–221, doi:10.1111/j.1365-3091.2006.00830.x.

Swenson, J. B., C. Paola, L. Pratson, V. R. Voller, and A. B. Murray (2005), Fluvial and marine controls on combined subaerial and subaqueous delta progradation: Morphodynamic modeling of compound-clinoform development, *J. Geophys. Res.*, *110*, F02013, doi:10.1029/2004JF000265.

Sylvia, D. A., and W. E. Galloway (2006), Morphology and stratigraphy of the late Quaternary lower Brazos valley: Implications for paleo-climate, discharge and sediment delivery, *Sediment. Geol.*, *190*(1–4), 159–175, doi:10.1016/j.sedgeo.2006.05.023.

Syvitski, J. P. M., and Y. Saito (2007), Morphodynamics of deltas under the influence of humans, *Global Planet. Change*, *57*(3–4), 261–282, doi:10.1016/j.gloplacha.2006.12.001.

Syvitski, J. P. M., et al. (2009), Sinking deltas due to human activities, *Nat. Geosci.*, *2*(10), 681–686, doi:10.1038/ngeo629.

Törnqvist, T. E., S. R. Wortman, Z. R. P. Mateo, G. A. Milne, and J. B. Swenson (2006), Did the last sea level lowstand always lead to cross-shelf valley formation and source-to-sink sediment flux?, *J. Geophys. Res.*, *111*, F04002, doi:10.1029/2005JF000425.

Tucker, G. E. (2004), Drainage basin sensitivity to tectonic and climatic forcing: Implications of a stochastic model for the role of entrainment and erosion thresholds, *Earth Surf. Processes Landforms*, *29*(2), 185–205, doi:10.1002/esp.1020.

Tucker, G. E., and R. Slingerland (1997), Drainage basin responses to climate change, *Water Resour. Res.*, *33*, 2031–2047, doi:10.1029/97WR00409.

United States Army Corps of Engineers (1935), Studies of river bed materials and their movements, with special reference to the lower Mississippi River, report, 161 pp., U.S. Waterw. Exp. Stn., Vicksburg, Miss.

Wang, F. C. (1984), The dynamics of a river-bay-delta system, *J. Geophys. Res.*, *89*, 8054–8060, doi:10.1029/JC089iC05p08054.

Whipple, K. X., G. S. Hancock, and R. S. Anderson (2000), River incision into bedrock: Mechanics and relative efficacy of plucking, abrasion, and cavitation, *Geol. Soc. Am. Bull.*, *112*(3), 490–503, doi:10.1130/0016-7606(2000)112<490:RIIBMA>2.0.CO;2.

Williams, G. P. (1978), Bankfull discharge of rivers, *Water Resour. Res.*, *14*, 1141–1154, doi:10.1029/WR014i006p01141.

Wolman, M. G., and J. P. Miller (1960), Magnitude and frequency of forces in geomorphic processes, *J. Geol.*, *68*, 54–74, doi:10.1086/626637.

Wright, L. D. (1977), Sediment transport and deposition at river mouths—Synthesis, *Geol. Soc. Am. Bull.*, *88*(6), 857–868, doi:10.1130/0016-7606(1977)88<857:STADAR>2.0.CO;2.

Wright, L. D., and J. M. Coleman (1971), Effluent expansion and interfacial mixing in the presence of a salt wedge, Mississippi River Delta, *J. Geophys. Res.*, *76*, 8649–8661, doi:10.1029/JC076i036p08649.

Wright, S., and G. Parker (2004), Flow resistance and suspended load in sand-bed rivers: Simplified stratification model, *J. Hydraul. Eng.*, *130*(8), 796–805, doi:10.1061/(ASCE)0733-9429(2004)130:8(796).

M. P. Lamb, Division of Geological and Planetary Sciences, California Institute of Technology, MC 170–25, 1200 E. California Blvd., Pasadena, CA 91125, USA. (mpl@gps.caltech.edu)

D. Mohrig and J. Shaw, Jackson School of Geosciences, University of Texas, 1 University Stn. C1100, Austin, TX 78712–0254, USA.

J. A. Nittrouer, Department of Geology, University of Illinois at Urbana-Champaign, 253 Natural History Bldg., Urbana, IL 61801, USA.

Erratum

In the originally published version of this article, equation 5 was incorrect. The equation has since been corrected and this version may be considered the authoritative version of record.

$$\frac{LS_b}{h_n} = \varsigma_L - \varsigma_s - \left(1 - F^2\right)[Z(\varsigma_L) - Z(\varsigma_s)], \qquad (5)$$